



Synthesis of epimer of Taniaphos ligand

Ambroz Almássy ^a, Erik Rakovský ^b, Andrea Malastová ^a, Zuzana Sorádová ^a, Radovan Šebesta ^{a,*}

^a Department of Organic Chemistry, Faculty of Natural Sciences, Comenius University in Bratislava, Mlynská dolina, Ilkovičova 6, 842 15 Bratislava, Slovakia

^b Department of Inorganic Chemistry, Faculty of Natural Sciences, Comenius University in Bratislava, Mlynská dolina, Ilkovičova 6, 842 15 Bratislava, Slovakia



ARTICLE INFO

Article history:

Received 14 July 2015

Received in revised form

1 December 2015

Accepted 8 January 2016

Available online 15 January 2016

Keywords:

Ferrocene

Directed *ortho*-metalation

Diastereoselective lithiation

Chiral ligand

Asymmetric catalysis

ABSTRACT

The spatial arrangement of groups within a chiral ligand is essential for its catalytic performance. This work describes convenient synthesis of (*R,S_p*)-1-(2-(diphenylphosphano)ferrocenyl)-1-(2-diphenylphosphanophenyl)-*N,N*-dimethylmethanamine, a diastereomer of the well known (*R,R_p*)-Taniaphos ligand. The compound was prepared from the same homochiral amine as Taniaphos by sequential twofold lithiation followed by trapping with diphenylphosphane chloride. Sequential twofold lithiation, in contrast to simultaneous dilithiation, leads to the opposite configuration of the stereogenic plane. The structure and configuration of the (*R,S_p*)-diastereomer along with its CuBr-complex were confirmed by X-ray structural analysis. DFT calculations elucidated underlying effects controlling the stereochemical outcome of the lithiation.

© 2016 Elsevier B.V. All rights reserved.

1. Introduction

Ferrocene is one of the prominent structural elements for building chiral ligands for asymmetric catalysis [1–6]. In particular, ferrocenyl phosphanes possessing elements of central and planar chirality represent an important group of ligands used in homogeneous asymmetric catalysis with transition metals [7,8]. Ferrocenyl phosphane, Taniaphos, introduced by Knochel and co-workers, is the highly useful type of chiral ligand [9]. Taniaphos proved helpful in the copper-catalyzed conjugate additions of organometallic reagents [10–18], copper-catalyzed allylic substitutions [19–22], or rhodium catalyzed hydrogenations [23–25].

Introduction and manipulation of stereogenic units during synthesis of chiral ferrocene ligands is an important topic [26]. Many chiral ferrocene ligands can be synthesized from suitable chiral amines. These homochiral α -amino derivatives often result from the resolution of corresponding racemic amines (Ugi's resolution) or stereoselective reduction of carbonyl compounds followed by a nucleophilic substitution with retention of the configuration. Stereoselective induction of the planar chirality is allowed by the *ortho*-directing amino group on α -carbon. Steric

control of the lithiation leads predominantly to (*R*,S*_p*)-relative configuration of the product (Scheme 1) [27,28].

In this transition state model, the hydrogen atom on α -carbon occupies the space between the planes of ferrocenyl Cp rings relieving the steric interaction of bulkier groups with the ferrocenyl fragment. These substituents on stereogenic center are located above the plane of the substituted Cp ring, and the introduction of lithium atom is directed by the nitrogen of the amino group. This model of the lithiation applies even in such constrained systems as *N,N*-dimethyl-[5]ferrocenophan-1'-amine [29].

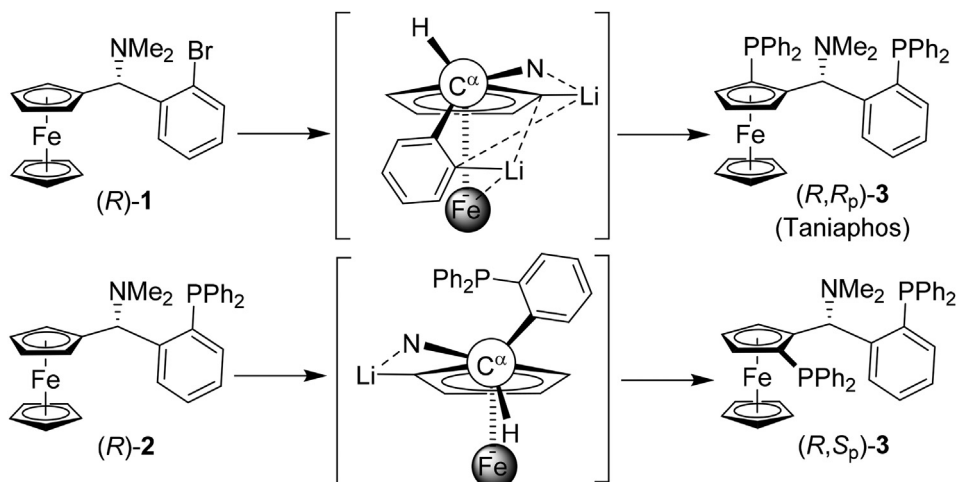
On the other hand, dilithiation of compound (R)-1 and subsequent reaction with PPh₂Cl leads to diphosphane (*R,R_p*)-3 (Taniaphos). The formation of a quasi-dimeric arrangement of lithium atoms in the transition state explains the configuration of the chiral plane (Scheme 1). Another factor, which further stabilizes this pathway may be an interaction of Li with Fe [30].

The presence of two lithium atoms in the transition state is essential to achieving the observed stereochemical result of the lithiation. Separating the lithiations in two distinct steps should, therefore, lead to the opposite configuration of the chiral plane similarly to other mono-lithiations.

Alternatively, Taniaphos-type ligands can also be synthesized by stereoselective *ortho*-lithiation of chiral ferrocenyl sulfoxides. Electrophilic quenching of the resulting Li-intermediate with 2-(diphenylphosphano)benzaldehyde provided two

* Corresponding author.

E-mail address: radovan.sebesta@fns.uniba.sk (R. Šebesta).

**Scheme 1.** Schematic representation of different course of double and step-wise lithiation.

diastereoisomeric alcohols with a different configuration of the chiral center on α -carbon formed in approximately equal amounts [31–34]. These alcohols were separated by chromatography and the sulfoxide group substituted with phosphano group. However, this method was not employed for the synthesis of (*R,S_p*)-configured diphosphane-amines [32].

In another approach, Fukuzawa and coworkers protected (*pro-S*) *ortho*-position of 1-ferrocenyl-*N,N*-dimethyl-1-phenylmethanamine with a trimethylsilyl group. Ensuing lithiation of the second *ortho*-position of Cp ring and phenyl ring helps to introduce two diphenylphosphano groups. After deprotection, they obtained (*R,R_p*)-Taniaphos [35,36].

In this context, we decided to investigate step-wise twofold lithiation for the synthesis of (*R,S_p*)-epimer of Taniaphos, compound (*R,S_p*)-3. To the best of our knowledge, the synthesis of diastereomer **3** was not accomplished, despite several attempts. We show that a careful control of reaction parameters enables one to perform the desired step-wise dilithiation and thus obtain epimer of Taniaphos.

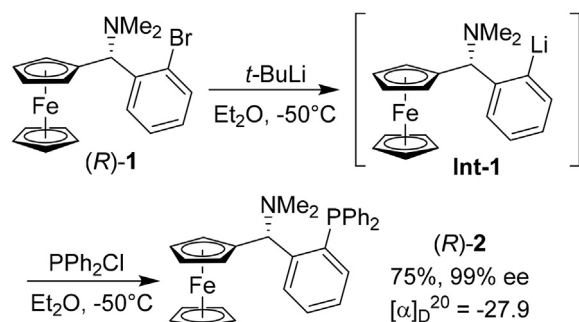
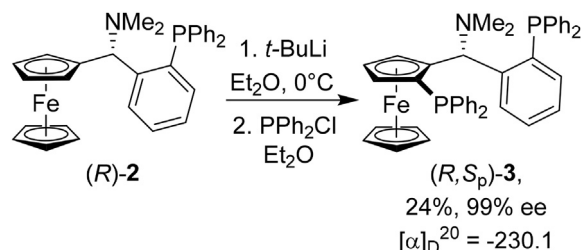
2. Results and discussion

2.1. Synthesis

Enantioselective CBS-reduction of (2-bromobenzoyl)ferrocene afforded the starting amine (*R*)-1. Crystallization of alcohol from heptane provided the corresponding product in 99% enantiomeric excess. The resulting alcohol was acetylated, and acetoxy group subsequently substituted for dimethylamino group following the procedure of Knochel and coworkers [9]. The nucleophilic substitution in the α -position to ferrocenyl moiety proceeds with complete retention of the configuration on the stereogenic center as was well documented in many ferrocenyl compounds.

Exposure of compound (*R*)-1 to *t*-BuLi resulted in an exchange of the bromine atom in *ortho*-position of the phenyl ring. This Br–Li exchange proceeded quickly even at low temperatures. Complete conversion of starting bromoamine **1** was achieved within one hour in THF at -50°C . Lithiated intermediate **Int-1** is moisture sensitive and decomposes by protolysis to the corresponding debrominated amine. To minimize this side reaction, the starting material (*R*)-1 should be dried carefully by heating above its melting point (m.p. 73°C) under vacuum [23]. Quenching of the reaction with PPh₂Cl afforded aminophosphane (*R*)-2 in 75% yield (Scheme 2).

The compound (*R*)-2 is an orange crystalline compound, which

**Scheme 2.** Synthesis of phosphane 2.**Scheme 3.** Synthesis of (*R,S_p*)-3.

slowly decomposes in chloroform solution forming the paramagnetic particles. Satisfactory ¹H, ¹³C, and ³¹P NMR spectra were recorded in *d*₆-acetone solution. The chemical shift of the phosphorus, a singlet at -17.2 ppm, is similar to that of the phenyl attached phosphorus in (*R,R_p*)-Taniaphos (doublet -16.7 ppm).

The subsequent lithiation of compound (*R*)-2 proceeded slowly (Scheme 3). It required elevated reaction temperature and longer time. Lithium was stereoselectively directed to the preferred *ortho*-position of the substituted Cp ring by coordination to the nitrogen atom of the amino group (see Scheme 1). Trapping of the corresponding lithiated intermediate **Int-2** with PPh₂Cl afforded the compound (*R,S_p*)-3. The ³¹P chemical shifts of phosphorus atoms in compound (*R,S_p*)-3 ($\delta = -18.1$ ppm for Ph-P and -27.0 ppm for Cp-P, *J*(P,P) = 39.6 Hz in CDCl₃ at 242.8 MHz) are similar to that of the phosphorus signals of diphosphane (*R,R_p*)-3 ($\delta = -16.7$ and -23.2 ppm, *J*(P,P) = 19.1 Hz in CDCl₃ at 81 MHz). Coupling with

both phosphorus atoms was observed on hydrogen H-C α ($J_{H,P} = 7.4$; 4.7 Hz in $CDCl_3$ at 600 MHz). Crystallization of the material from $CHCl_3$ /heptane mixture afforded the sample suitable for X-ray crystallographic analysis.

Zheng et al. reported preparation of Taniaphos ligand from α -ferrocenylbenzyl-*N,N*-dimethylamine [37]. The reported synthesis consisted of two distinct lithiation steps each followed by reaction with PPh_2Cl . In that case, however, the first diphenylphosphanyl group was introduced stereoselectively on the substituted Cp ring by the directed *ortho*-lithiation resulting in phosphano-amine as described by Yamamoto and co-workers [38]. The absolute configuration of the product was determined by comparing of CD spectra with related compounds and later was confirmed in our laboratory by X-ray crystallographic analysis. While the absolute configuration of this compound remains the same during the next *ortho*-lithiation of the phenyl ring, the formation of diphosphane (R,S_p)-3 should be expected. However, we could not obtain neither diphosphane (R,R_p)-3, nor diphosphane (R,S_p)-3 by this procedure. We attempted the lithiation of the compound with *n*-BuLi, *s*-BuLi or *t*-BuLi, respectively, and subsequent reaction with chlorophosphane.

2.2. Structural characterization

Compound (R,S_p)-3 crystallizes in space group $P2_12_12_1$ (Supporting information, Figs. S1 and S2). The molecule has the (*R*)-configuration on C15 and (S_p)-configuration of the stereogenic plane. Intermolecular interaction are based on dispersive forces, predominantly C–H ... π interactions; however, based on X-ray data, there are no interactions shorter than the sum of VdW radii found.

The dihedral angle of the Cp rings is 2.9°. Fe to Cp distances are 1.65 Å and 1.66 Å for C1–C5 and C6–C10 rings, respectively.

The absolute structure was determined from anomalous dispersion effects using Friedel difference restraints for obtaining better convergence of Flack *x* parameter [39,40]. Hooft *y* parameter obtained with *x* set to 0 is −0.016(6). Both *x* and *y* values indicate correct handedness and enantiopurity (Fig. 1) [41].

Taniaphos type ligands can coordinate on the transition metals by two phosphorus and one nitrogen atom [42,43]. For the demonstration of coordination ability of the ligand (R,S_p)-3 complex of CuBr with homochiral (R,S_p)-3 was prepared and

structurally characterized. The appropriate X-ray crystallographic sample was obtained by crystallization from $CHCl_3$ /hexane. The complex $[Cu(R,S_p\text{-}3)\text{Br}]$ is a stable yellow crystalline compound. Chiu and coworkers described the structure of the corresponding diastereomeric complex $[Cu(R,R_p\text{-}3)\text{Br}]$ [43]. Both ligands coordinate the central copper atom by both phosphorus atoms forming an eight-membered metallacycle. In the $[Cu(R,S_p\text{-}3)\text{Br}]$, bite angle 127.7° is wider in comparison with Cu-complex of Taniaphos 114.7°. The Cu–Br bond in complex $[Cu(R,S_p\text{-}3)\text{Br}]$ (2.34 Å) is perpendicular to the axis of the ferrocene fragment and is directed in the plane of the ring. On the other hand, the metallacycle is more bend in the Taniaphos complex, and the Cu–Br bond (2.32 Å) is almost parallel to the axis of ferrocene fragment. Compound $[Cu(R,S_p\text{-}3)\text{Br}]$ crystallizes in $P2_12_12_1$ (Supporting information, Figs. S3 and S4). The molecule has (*R*)-configuration on C6 and (S_p)-configuration of the stereogenic plane. The intermolecular interactions are predominantly based on weak C–H ... N and C–H ... Br interactions (Table 1) with some contribution of C–H ... π interactions [44]. The structure contained solvent-accessible voids with the total volume of 223.4 Å³ (5.9% of the cell volume). By using solvent masking technique, we revealed that these voids are empty (electron population 0.0) [45].

The dihedral angle between Cp rings is 6.5(3)°. Fe to Cp distance is 1.64 Å from C1–C5 ring and 1.66 Å from C1A–C5A ring.

The absolute structure was determined from anomalous dispersion effects by post-refinement Flack *x* factor calculation using Parson's quotients [46]. Hooft *y* parameter obtained with *x* set to 0 is 0.008(6). Based on both parameters, the compound $[Cu(R,S_p\text{-}3)\text{Br}]$ is also enantiopure, and the absolute structure is determined with correct handedness (Fig. 2).

We have also measured CD spectra of both diastereomers (R,R_p) and (R,S_p)-3. These spectra suggest that the planar stereogenic unit is a dominant element of chirality (Fig. 3).

2.3. DFT calculations

Quantum chemical calculations helped elucidate underlying reasons for the observed stereoselectivity of the lithiation. Steric interactions govern the stereochemical course of the lithium atom introduction to the Cp-ring.

The double lithiation, which is employed in the synthesis of Taniaphos ligand ((R,R_p)-3), proceeds preferentially to the *pro-S_p* position due to the formation of dilithium arrangement in the transition state. Another reason helping reverse the course of the lithiation may be an interaction of Fe with one of the lithium atoms [30]. Fig. 4 depicts the reaction coordinate for the lithiation of phosphane (*R*)-2. The reaction starts with complex formation between ferrocene derivative (*R*)-2 and the base *t*-BuLi. There are two conformers of the starting complex. These conformers lead to two transition states (*pro-R_p*) and (*pro-S_p*). The *t*-BuLi coordinated by lithium to both nitrogen and phosphorus attacks the acidic hydrogen of the ferrocene. The presence of bulky diphenylphosphanyl group at the benzyl moiety and the fact that lithium is coordinated to phosphorus brings the benzene groups closer to the reaction center. These factors make the transition states rather sterically hindered. In the (*pro-S_p*) transition state, the phenyl

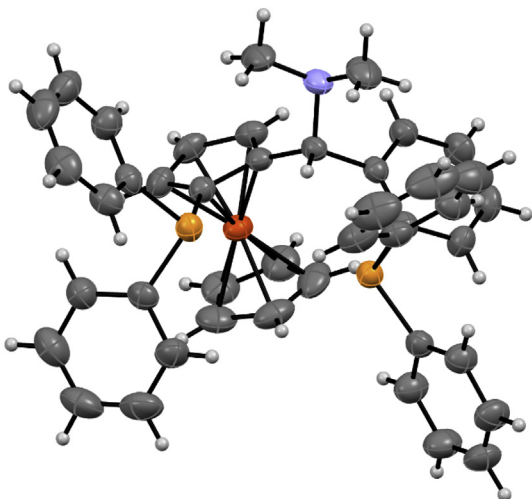


Fig. 1. X-ray crystallographic structure of (R,S_p)-3. Thermal ellipsoids were drawn at 30% probability level.

Table 1
Selected intermolecular interactions in the crystal structure of $[Cu(R,S_p\text{-}3)\text{Br}]$.

	$d(C\text{--}H)$ [Å]	$d(H\text{--}A)$ [Å]	$d(D\text{...}A)$ [Å]	$D\text{--}H\text{...}A$ [°]
C5A–H5A ... N1 ⁱ	0.93	2.85	3.724(9)	157.1
C15–H15 ... Br1 ⁱⁱ	0.93	3.03	3.850(8)	148.0
C29–H29 ... Br1 ⁱⁱ	0.93	3.07	3.781(8)	134.4

Symmetry operations: i = ($\frac{1}{2} + x, \frac{1}{2} - y, 1 - z$), ii = ($-\frac{1}{2} + x, 3/2 - y, 1 - z$).

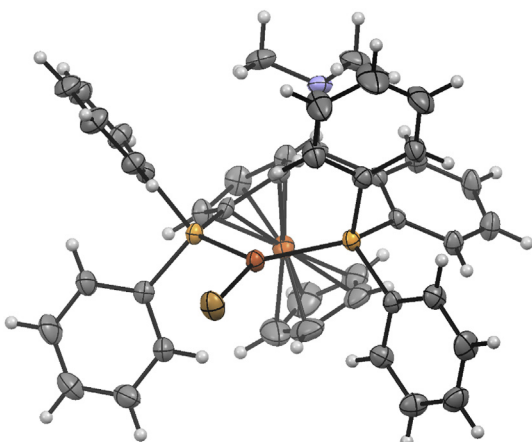


Fig. 2. X-ray crystallographic structure of $[\text{Cu}(\text{R},\text{S}_p)\text{-3}]\text{Br}$. Thermal ellipsoids were drawn at 30% probability level.

intermediates. The solvent stabilizes the lithium of intermediates that results in more stable structures.

2.4. Catalytic activity

The catalytic activity of ligand $(\text{R},\text{S}_p)\text{-3}$ in transition metal homogeneous catalysis was demonstrated on stereoselective Rh-catalyzed hydrogenation of dimethyl itaconate. These preliminary results were compared with those obtained using Rh complex of Taniaphos ligand $(\text{R},\text{R}_p)\text{-3}$. Conversion of the starting material **4** was complete after 24 h in both cases. The ligand $(\text{R},\text{R}_p)\text{-3}$ provided the corresponding hydrogenation product, (*S*)-2-methylsuccinate dimethyl ester (**5**) with 91% ee. The epimeric ligand $(\text{R},\text{S}_p)\text{-3}$ afforded this product with opposite (*R*)-configuration but only in 21% ee. These experiments show that the configuration of the ligands chiral plane has a major influence on the stereoselective outcome of the reduction (see Scheme 4).

We have also tested both epimers of diphosphane **3** in the Cu-

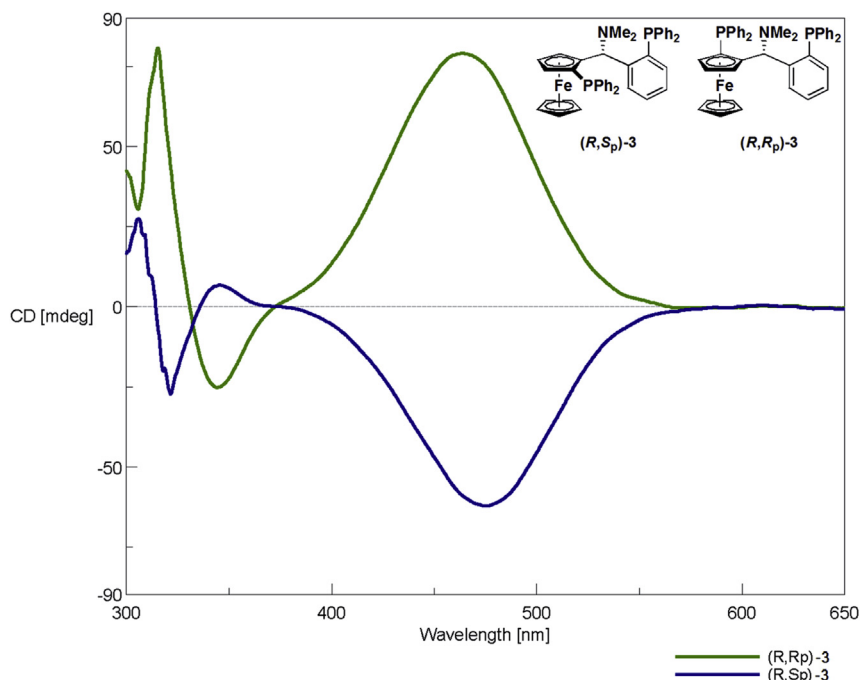


Fig. 3. CD spectra of compounds (R,S_p) and $(\text{R},\text{R}_p)\text{-3}$.

groups of the PPh_2 group are located over the Cp-ring. In fact, one of these phenyls lies parallel with the Cp-ring of the ferrocene moiety. While in (*pro-R_p*) transition state, two phenyl groups are oriented towards the ferrocene skeleton that disfavors the formation of the (*pro-R_p*) transition state. NCI visualization demonstrates these repulsions (Fig. 5). The lithiation reaction results in the formation of stable intermediates **Int-2**. Energies of these intermediates are very similar.

Calculated energies for the lithiation of (*R*)-**2** with *t*-BuLi are summarized in Table 2. The energy difference between (*pro-S_p*)-TS and (*pro-R_p*)-TS is 10 kJ/mol. This energy difference would correspond to Boltzmann distribution of products about 98:2. The inclusion of the solvation effect of Et_2O leads to higher activation barrier of the reaction, but the energy difference between diastereomeric transition states remains the same. The positive influence of solvation effect can be observed in energies of formed

catalyzed enantioselective conjugate addition of ethylmagnesium bromide to enones (Scheme 5). A similar trend to the Rh-catalyzed hydrogenation was observed. Copper complexes with both epimers promoted the reaction with full conversion. However, the ligand $(\text{R},\text{S}_p)\text{-3}$ afforded the corresponding adducts **7a-c** in low enantiomeric purities, and with opposite absolute configuration than $(\text{R},\text{R}_p)\text{-3}$ (Taniaphos). The results of Cu-catalyzed conjugate additions are summarized in Table 3.

To elucidate the difference in catalytic performance between $(\text{R},\text{R}_p)\text{-3}$ and $(\text{R},\text{S}_p)\text{-3}$ in the Rh-catalyzed hydrogenation, we also prepared its Rh-complex. The complex $[\text{Rh}(\text{R},\text{S}_p)\text{-3}\text{COD}]\text{BF}_4$ was characterized by ^1H , ^{13}C , and ^{31}P NMR, however, we were not able to characterize it by X-ray crystallography. Therefore, its 3-D structure was obtained by DFT calculations. This structure was then compared with X-ray structure of Rh-Taniaphos obtained by Knochel [9]. Rhodium atom in Taniaphos complex is more tightly

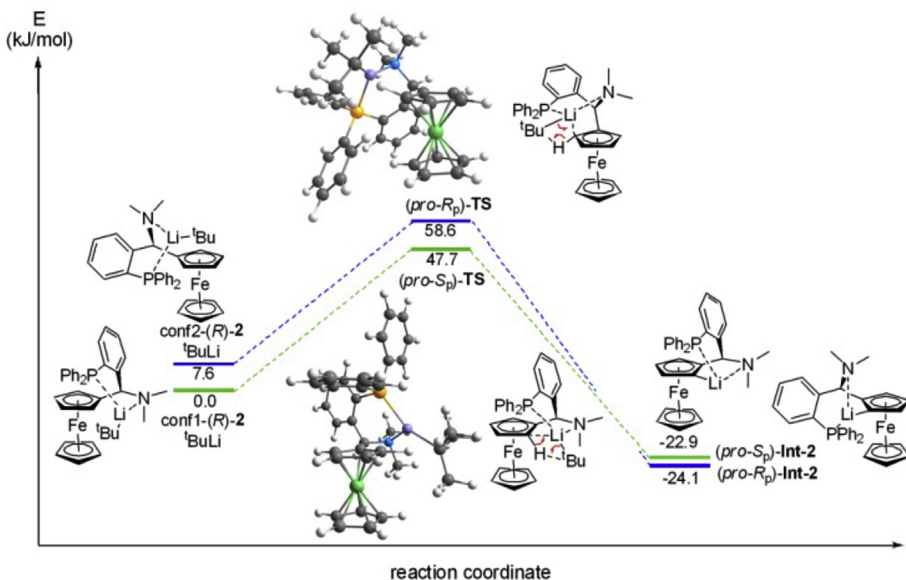


Fig. 4. Reaction coordinate for the lithiation of (R)-2.

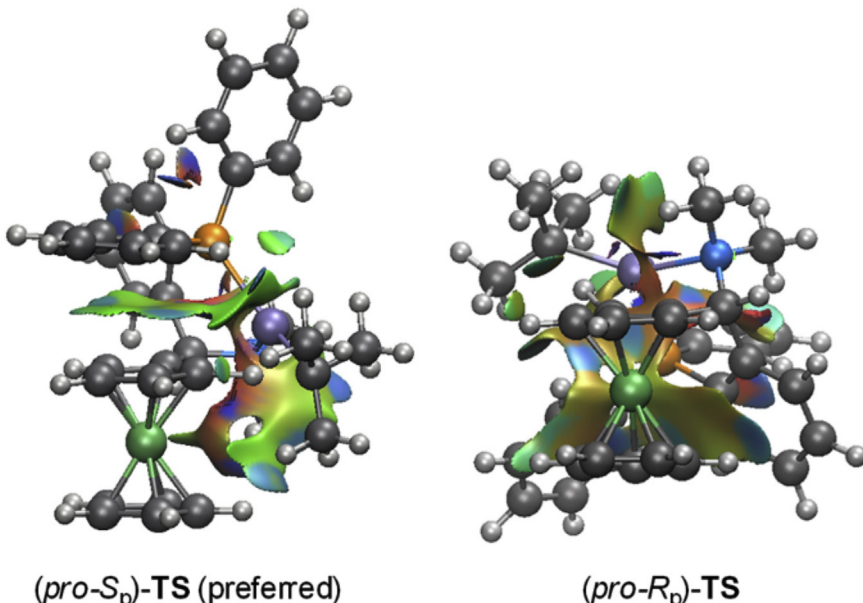
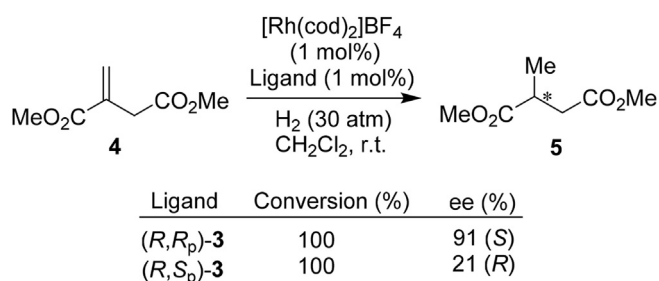


Fig. 5. NCI plot of the transition states.

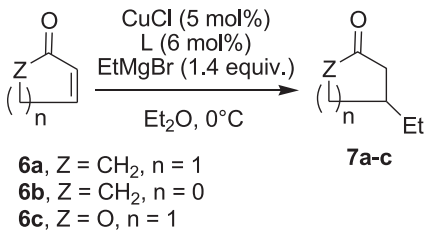
Table 2
Calculated energies for lithiation of (R)-2.

Compound	ΔE (kJ/mol)	ΔE^a (kJ/mol)
Conf1-(R)-2 · t-BuLi	0.0	0.0
Conf2-(R)-2 · t-BuLi	10.9	7.6
(pro-S _p)-TS	40.0	47.7
(pro-R _p)-TS	50.1	58.6
(pro-S _p)-Int-2	-11.2	-22.9
(pro-R _p)-Int-2	-16.3	-24.1

^a The solvent (Et_2O) is included.

Scheme 4. Rh-catalyzed hydrogenation of **4** using (*R,R_p*)-3 and (*R,S_p*)-3.

surrounded by neighboring groups (ferrocene moiety, phenyl groups on the phosphorus and NMe_2). On the other hand in the ep-Taniaphos complex, these groups seem to be further away (Fig. 6).



Scheme 5. Cu-catalyzed conjugate addition of EtMgBr to enones using (*R,R_p*) and (*R,S_p*)-3.

Table 3
Cu-Catalyzed conjugate addition of EtMgBr to enones.^a

Enone	Ligand	Conversion (%) ^b	ee of 7a-c (%) ^c
6a	(<i>R,R_p</i>)-3	100	82 (R)
	(<i>R,S_p</i>)-3	100	6 (S)
6b	(<i>R,R_p</i>)-3	100	4 (R)
	(<i>R,S_p</i>)-3	95	2 (S)
6c	(<i>R,R_p</i>)-3	100	12(R)
	(<i>R,S_p</i>)-3	100	4 (S)

^a Reaction was performed with CuCl (5 mol%), Ligand (6 mol%), EtMgBr (140 mol%).

^b Determined by GC.

^c Determined by chiral GC.

4. Experimental section

4.1. Synthesis of phosphane (*R*)-2

To the solution of amine (*R*)-1 (375 mg, 0.94 mmol) in dry degassed Et₂O (10 mL) was added 1.6 M solution of *t*-BuLi in pentane (890 μ L, 1.41 mmol) dropwise at -60 °C. Mixture was stirred at -50 °C for 45 min. Neat distilled PPh₂Cl (290 μ L, 1.6 mmol) was added dropwise at -50 °C. Mixture was stirred at RT for 16 h. 5% NaHCO₃ aq. soln. (3 mL) was added and layers were separated. Aqueous layer was extracted with Et₂O (3 \times 8 mL). Combined organic layers were washed with water (2 \times 8 mL) and brine (8 mL). The product was isolated by flash chromatography (SiO₂, hexanes/EtOAc 3:1 + 1% Et₃N) as 356 mg (75%) of orange oil. Product was recrystallized from MeOH. $[\alpha]_D^{20} = -27.9$ ($c = 0.615$, *t*-BuOMe). ¹H NMR (*d*₆-acetone, 600 MHz, 20 °C, TMS): $\delta = 7.78$ (ddd, $J = 7.8$ Hz, $J = 4.4$ Hz, $J = 1.2$ Hz, 1H, H-C^{Ph}), 7.33–7.48 (m, 11H, H-C^{Ph}), 7.24 (ddd, $J = 7.5$ Hz, $J = 7.5$ Hz, $J = 1.3$ Hz, 1H, H-C^{Ph}), 7.11 (ddd, $J = 7.7$ Hz, $J = 3.8$ Hz, $J = 1.2$ Hz, 1H, H-C^{Ph}), 5.05 (d, $J_{C,P} = 8.0$ Hz, 1H, H-C²), 4.25–4.28 (m, 1H, H-C^{Fc}), 4.16–4.18 (m, 1H, H-C^{Fc}), 4.12–4.15 (m, 2H, H-C^{Fc}), 3.79 (s, 5H, Cp), 1.77 (s, 6H, NMe₂) ppm. ¹³C NMR (*d*₆-acetone, 150.8 MHz, 20 °C, TMS): $\delta = 149.5$ ($J_{C,P} = 22.4$ Hz), 138.0

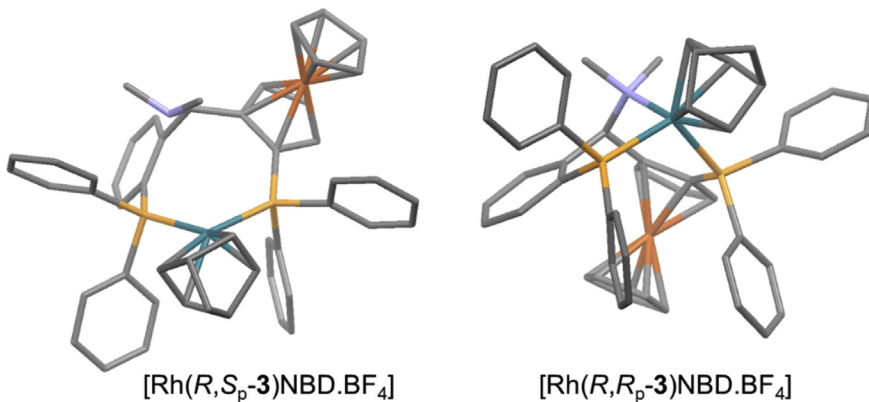


Fig. 6. Structures of Rh-complexes with (*R,S_p*) and (*R,R_p*)-3.

This fact likely means that the chiral environment around the Rh is less well defined. During the catalytic reaction, a few orientations of the substrate are probably possible, thus leading to lower enantioselectivity.

3. Conclusions

Step-wise di-lithiation of amine **1** proceeds with the different stereochemical course than simultaneous dilithiation. The presence of lithium atom on phenyl ring participates in the formation of Li-dimeric species and also interacts with iron, and this is only possible in the *ortho*-lithiation to (*pro-R_p*)-position of the Cp-ring. On the other hand, sequential dilithiation is controlled only sterically by introducing the lithium into (*pro-S_p*) position on the Cp-ring. This feature enables synthesis of (*R,S_p*)-epimer of Taniaphos ligand, which was not accessible easily so far. X-ray crystallography confirmed the absolute configuration of the ligand (*R,S_p*)-3 and its coordination to copper. DFT calculations helped elucidate the stereochemical course of the lithiation. In the Rh-catalyzed hydrogenation, diastereomers of **3** afforded product with the opposite configuration, which means that the planar stereogenic unit of the ligand controlled stereochemical outcome of the hydrogenation.

($J_{C,P} = 13.3$ Hz), 137.4 ($J_{C,P} = 10.3$ Hz), 136.1 ($J_{C,P} = 13.8$ Hz), 134.0, 133.9, 133.8, 133.7, 128.9 ($J_{C,P} = 4.8$ Hz), 128.7, 128.6, 128.5, 128.4 ($J_{C,P} = 7.3$ Hz), 126.7, 90.8, 70.1, 68.7, 67.7, 67.3, 66.4 ($J_{C,P} = 23.0$ Hz), 65.8, 42.7 ppm. ³¹P NMR (*d*₆-acetone, 242.8 MHz, 20 °C): $\delta = -17.2$ ppm. MS (*m/z*): 459.0 [M – NMe₂]⁺.

4.2. Synthesis of diphosphane (*R,S_p*)-2

To the solution of phosphane (*R*)-2 (155 mg, 0.31 mmol) in dry degassed Et₂O (4 mL) was added 1.6 M solution of *t*-BuLi in pentane (670 μ L, 0.79 mmol) dropwise at -50 °C. The mixture was stirred for 2.5 h while the temperature rose to 0 °C. The solution was stirred at 0 °C for another 2 h then cooled to -30 °C and neat PPh₂Cl (95 μ L, 0.53 mmol) was added. After heating to RT, the reaction was quenched with 5% NaHCO₃ aq. soln. (1.5 mL). Layers were separated, and the aqueous layer was extracted with 1% solution of Et₃N in DCM (3 \times 3 mL). Combined organic parts were dried over Na₂SO₄ and evaporated. The product was isolated by flash chromatography (SiO₂, hexanes/EtOAc 8:1 + 1% Et₃N) as 50.2 mg (24%) of orange solid.

$[\alpha]_D^{20} = -230.1$ ($c = 0.900$, CHCl₃). ¹H NMR (CDCl₃, 600 MHz, 20 °C, TMS): $\delta = 7.83$ –7.88 (m, 1H, H-C^{Ph}), 7.63–7.69 (m, 2H, H-C^{Ph}),

Table 4Experimental data for (*R,S_p*)-**3** and [Cu(*R,S_p*-**3**)Br].

Empirical formula	C ₄₃ H ₃₉ FeNP ₂ ((<i>R,S_p</i>)- 3)	C ₄₃ H ₃₉ BrCuFeNP ₂ ([Cu(<i>R,S_p</i> - 3)Br])
CCDC No.	951497	1003402
M _r	687.58	830.99
Crystal system, space group	Orthorombic, P212121	Orthorombic, P212121
Unit cell dimensions	determined from 23972 reflections	determined from 11739 reflections
a [Å], α [°]	10.7370(2), 90	10.2549(4), 90
b [Å], β [°]	15.1527(3), 90	16.7919(7), 90
c [Å], γ [°]	21.5290(4), 90	21.9178(9), 90
V [Å ³]	3502.64(12)	3774.2(3)
Z, Z'	4, 1	4, 1
μ[mm ⁻¹], ρ (calcd.) [g cm ⁻³]	0.554, 1.304	2.123, 1.462
F(000)	1440	1696
Absorption correction, T _{min} , T _{max}	Analytical, 0.574, 0.893	Gaussian integration with beam profile correction, 0.498, 0.686
Crystal size [mm]	1.38 × 0.37 × 0.31	0.48 × 0.36 × 0.24
Crystal habit, color	Prism, yellow	Block, orange
θ range for data collection [°]	2.998–26.371	2.506–26.372
Limiting indices	<i>h</i> = -13 → 13 <i>k</i> = -18 → 18 <i>l</i> = -26 → 26	<i>h</i> = -12 → 11 <i>k</i> = -17 → 20 <i>l</i> = -27 → 26
Reflections collected/unique/observed	68302/7149/6750	19545/7671/6038
[<i>I</i> > 2σ(<i>I</i>)]	[R _{int} = 0.035, Friedel opposites not merged]	[R _{int} = 0.061, Friedel opposites not merged]
Completeness to θ [°]	99.8%–26.371°	99.8%–26.372°
Data/restraints/parameters	7149/2160/425	7671/544/444
Final weighting scheme	w = 1/[σ ² (F _o ²) + (0.04P) ² + 0.99P] where P = [max(F _o ² , 0) + 2F _c ²]/3	w = 1/[σ ² (F _o ²) + (0.0571P) ² + 0.2505P] where P = (F _o ² + 2F _c ²)/3
Absolute structure determination	From anomalous dispersion effects 3453 Friedel pairs using 2161 difference restraints Flack x factor -0.0036(18)	From anomalous dispersion effects 3370 Friedel pairs using 2258 quotients Flack x factor -0.008(7)
S (goodness-of-fit)	1.0134	1.030/1.033 (restrained)
Final R indices [<i>I</i> > 2σ(<i>I</i>)]	R = 2.96%, wR = 7.37%	R = 4.36%, wR = 9.98%
Final R indices (all data)	R = 3.22%, wR = 7.61%	R = 6.28%, wR = 10.91%
Largest difference peak/hole [e Å ⁻³]	0.53/−0.36	0.598/−0.445

7.46–7.57 (m, 4H, H-C^{Ph}), 7.29–7.46 (m, 11 H, H-C^{Ph}), 7.16–7.28 (m, 6H, H-C^{Ph}), 5.39–5.47 (dd, J_{H,P} = 7.4 Hz, J_{H,P} = 4.7 Hz, 1H, H-C^α), 4.62–4.72 (m, 1H, H-C^{Fc}), 4.36–4.41 (m, 1H, H-C^{Fc}), 4.08–4.11 (m, 1H, H-C^{Fc}), 3.36 (s, 5H, Cp), 1.53 (s, 6H, NMe₂) ppm. ¹³C NMR (CDCl₃, 150.8 MHz, 20 °C, TMS): δ = 149.8 (J_{C,P} = 24.8 Hz), 140.5 (J_{C,P} = 10.6 Hz), 139.7 (J_{C,P} = 12.0 Hz), 137.7 (J_{C,P} = 14.4 Hz), 136.6 (J_{C,P} = 16.9 Hz), 135.3 (J_{C,P} = 22.0 Hz), 134.7 (J_{C,P} = 20.0 Hz), 134.2, 134.1 (J_{C,P} = 19.1 Hz), 132.9 (J_{C,P} = 18.9 Hz), 128.7, 127.1 (J_{C,P} = 64.7 Hz), 132.6 (J_{C,P} = 18.0 Hz), 128.7, 128.5 (J_{C,P} = 6.5 Hz), 128.4 (J_{C,P} = 39.6 Hz), 128.3 (J_{C,P} = 14.0 Hz), 127.8 (J_{C,P} = 7.9 Hz), 127.6 (J_{C,P} = 5.9 Hz), 127.4 (J_{C,P} = 64.6 Hz), 70.6 (br s), 70.1, 69.9, 69.5 (br s), 64.7 (br s), 44.0 ppm. ³¹P NMR (CDCl₃, 242.8 MHz, 20 °C): δ = -18.1 (d, J_{P,P} = 39.6 Hz), -27.0 (d, J_{P,P} = 39.6 Hz) ppm. MS (m/z): 643.3 [M - NMe₂]⁺.

4.3. Synthesis of complex [Cu(*R,S_p*-**3**)Br]

A mixture of ligand (*R,S_p*)-**3** (6.7 mg, 0.01 mmol), CuBr.Me₂S (2.0 mg, 0.01 mmol) and dry CH₂Cl₂ (1.5 mL, neutralized by passing through the short basic alumina pad), was stirred for 1 h at RT until the white cuprous salt dissolved. The solvent was evaporated under vacuum, and the yellow precipitate was recrystallized from CH₂Cl₂/hexane to yield 6.2 mg (81%) of yellow crystals. The crystallographic sample was obtained by recrystallization from CHCl₃/hexane.

¹H NMR (CDCl₃, 600 MHz, 20 °C, TMS): δ = 8.03–7.88 (m, 3H, H-C^{Ph}); 8.01–7.97 (m, 1H, H-C^{Ph}); 7.95–7.89 (m, 2H, H-C^{Ph}); 7.86–7.81 (m, 2H, H-C^{Ph}); 7.81–7.76 (m, 2H, H-C^{Ph}); 7.58–7.52 (m, 10H, H-C^{Ph}); 7.42–7.37 (m, 1H, H-C^{Ph}); 7.37–7.31 (m, 5H, H-C^{Ph}); 7.14–7.09 (m, 1H, H-C^{Ph}); 5.27–5.21 (m, 1H, HCN); 4.83–4.77 (m, 1H, H-C^{Fc}); 4.47–4.44 (m, 1H, H-C^{Fc}); 4.04–4.00 (m, 1H, H-C^{Fc}); 3.51 (s, 5H, Cp); 1.28 (s, 6H, NMe₂) ppm. ¹³C NMR (CDCl₃, 150.8 MHz, 20 °C, TMS): δ = 151.1 (J_{C,P} = 14.8 Hz), 135.6 (J_{C,P} = 15.3 Hz), 135.3 (J_{C,P} = 15.6 Hz), 134.0 (J_{C,P} = 14.0 Hz), 133.8, 133.6 (J_{C,P} = 14.7 Hz), 131.8, 131.6, 131.5,

131.4, 130.8 (J_{C,P} = 15.4 Hz), 130.4, 130.0, 129.8 (J_{C,P} = 9.2 Hz), 129.0 (J_{C,P} = 9.4 Hz), 128.9 (J_{C,P} = 5.2 Hz), 128.8 (J_{C,P} = 8.8 Hz), 128.4 (J_{C,P} = 6.9 Hz), 128.4 (J_{C,P} = 6.0 Hz), 127.3 (J_{C,P} = 5.0 Hz), 98.7 (J_{C,P} = 20.3 Hz), 71.3, 71.2, 70.7 (J_{C,P} = 4.0 Hz), 70.3 (C₅H₅), 63.8, 44.8 (N-(CH₃)₂) ppm. ³¹P NMR (CDCl₃, 242.8 MHz, 20 °C): δ = -12.2 (d, J_{P,P} = 150 Hz); -18.8 (d, J_{P,P} = 150 Hz) ppm.

4.4. Synthesis of complex [Rh(*R,S_p*-**3**)cod.BF₄]

To the solution of ligand (*R,S_p*)-**3** (12.3 mg, 0.18 mmol) in dry CH₂Cl₂ (1.5 mL) was added [Rh(cod)₂]BF₄ (7.3 mg, 0.18 mmol). The mixture was stirred for 2 h at RT. Product was precipitated by addition of hexane. Orange crystals were filtered off and washed with hexane. Product was recrystallized from CH₂Cl₂/hexane.

¹H NMR (CDCl₃, 600 MHz, 20 °C, TMS): δ = 8.19–8.27 (m, 1H), 7.90–8.02 (m, 2H), 7.64–7.77 (m, 4H), 6.88–7.49 (m, 17H), 6.26–6.41 (m, 2H), 5.82–5.92 (m, 1H), 5.23–5.29 (m, 1H), 3.82–3.69 (m, 2H), 3.45 (s, 5H, Cp), 1.90–2.90 (m, 8H), 2.63 (s, 6H, NMe₂) ppm. ¹³C NMR (CDCl₃, 150.8 MHz, 20 °C, TMS): δ = 155.6, 155.4, 138.0, 137.2, 136.6, 133.9, 133.5, 133.3, 132.4, 132.1, 131.2, 130.8, 130.0, 129.9, 129.5, 129.3, 129.1, 128.9, 128.9, 128.7, 128.2, 128.1, 127.4, 127.3, 126.8, 126.7, 105.1, 104.9, 74.4, 73.8, 73.3, 71.9, 71.3, 70.8, 70.6, 70.3, 70.2, 69.1, 69.0, 46.6, 31.9, 30.4 ppm. ³¹P NMR (CDCl₃, 242.8 MHz, 20 °C): δ = 13.0 (dd, J_{Rh,P} = 136.9 Hz, J_{P,P} = 18.6 Hz), 10.6 (dd, J_{Rh,P} = 138.8 Hz, J_{P,P} = 18.6 Hz) ppm.

4.5. X-ray structure determination

The intensity data for (*R,S_p*)-**3** and [Cu(*R,S_p*-**3**)Br] were collected on a Kuma KM-4 CCD κ-axis diffractometer using graphite-monochromated MoKα radiation (0.71073 Å) at room temperature (293 K). The diffraction intensities were corrected for Lorentz, polarization and absorption effects. Data collection, cell refinement,

data reduction and finalization including all corrections mentioned above were carried by CrysAlis Pro software [47].

The structures were solved by charge flipping using olex2.solve (Olex2 ver. 1.2.5) [48].

The structure of (*R,S_p*)-3 were refined by CRYSTALS (ver. 14.40) [49]. All non-H atoms were refined anisotropically with free coordinates. The H atoms were localized in difference density map and refined using soft restraints on bond length and angles ($d(C-H) = 0.93\text{--}0.98 \text{ \AA}$) to regularize geometry; in the final cycles of the refinement, riding constraints were used [50]. $U_{\text{iso}}(\text{H})$ were constrained to the U_{eq} of the parent atoms with $U_{\text{iso}}(\text{H}) = 1.2U_{\text{eq}}(\text{C}_{\text{sp}2})$ and $U_{\text{iso}}(\text{H}) = 1.5U_{\text{eq}}(\text{C}_{\text{sp}3})$.

The structure of [Cu(*R,S_p*-3)Br] was refined by SHELXL-2014 [51]. All non-H atoms were refined anisotropically with free coordinates. Due to the motion disorder of C1A–C5A *Cp* ring, ADP and distance similarity restraints (SIMU and SADI) were applied to the atoms mentioned; rigid bond (RIGU) restraints for whole molecule to improve data-to-parameter ratio were also applied. All aromatic H atoms were placed into idealised positions with riding coordinates and $U_{\text{iso}} = 1.2U_{\text{eq}}(\text{C}_{\text{sp}2})$ [for disordered H1A–H5A atoms, $U_{\text{iso}} = 1.5U_{\text{eq}}(\text{C}_{\text{sp}2})$ were used]. Methyl groups were refined as freely rotating group with $U_{\text{iso}}(\text{H}) = 1.5U_{\text{eq}}(\text{C}_{\text{sp}3})$.

Hooft y parameter was calculated by CRYSTALS ((*R,S_p*)-3) and Olex2 ([Cu(*R,S_p*-3)Br]) using Gaussian distribution. The geometrical analysis was performed using SHELXL-2014 and Olex2; Olex2 was also used for structural drawings. Crystal data and conditions of the data collection and refinement are reported in Table 4.

Notes

The deposition number CCDC 951497 ((*R,S_p*)-3) and CCDC 1003402 ([Cu(*R,S_p*-3)Br]) contains the supplementary crystallographic data for this paper (including structure factors). These data can be obtained free of charge via www.ccdc.cam.ac.uk/data_request/cif or Cambridge Crystallographic Data Centre, 12 Union Road, Cambridge CB2 1EZ, UK; fax: +44 1223 336033.

Acknowledgments

For financial support, we thank the Slovak Research and Development Agency, grant no. APVV-0321-12, and Slovak Grant Agency VEGA, grant no. 1/0623/12 and 1/0336/13. This publication is the result of the project implementation: 26240120025 supported by the Research & Development Operational Programme funded by the European Regional Development Fund.

Appendix A. Supplementary data

Supplementary data related to this article can be found at <http://dx.doi.org/10.1016/j.jorgchem.2016.01.004>.

References

- [1] L.-X. Dai, X.-L. Hou, *Chiral Ferrocenes in Asymmetric Catalysis*, Wiley-VCH, Weinheim, 2010.
- [2] P. Štepníčka, *Ferrocene: Ligands, Materials and Biomolecules*, Wiley, Chichester, 2008.
- [3] R.G. Arrayas, J. Adrio, J.C. Carretero, Recent applications of chiral ferrocene ligands in asymmetric catalysis, *Angew. Chem. Int. Ed.* 45 (2006) 7674–7715.
- [4] N.A. Butt, D. Liu, W. Zhang, The design and synthesis of planar chiral ligands and their application to asymmetric catalysis, *Synlett* 25 (2014) 615–630.
- [5] Y. Miyake, Y. Nishibayashi, S. Uemura, Optically active chiral ligands, ferrocenylloxazolinylphosphines (FOXAPs): development and application to catalytic asymmetric reactions, *Synlett* (2008) 1747–1758.
- [6] R.C.J. Atkinson, V.C. Gibson, N.J. Long, The syntheses and catalytic applications of unsymmetrical ferrocene ligands, *Chem. Soc. Rev.* 33 (2004) 313–328.
- [7] M. Drusan, R. Šebesta, Enantioselective C-C and C-heteroatom bond forming reactions using chiral ferrocene catalysts, *Tetrahedron* 70 (2014) 759–786.
- [8] T.J. Colacot, A concise update on the applications of chiral ferrocenyl phosphines in homogeneous catalysis leading to organic synthesis, *Chem. Rev.* 103 (2003) 3101–3118.
- [9] T. Ireland, G. Grossheimann, C. Wieser-Jeunesse, P. Knochel, Ferrocenyl ligands with two phosphanyl substituents in the α,ϵ positions for the transition metal catalyzed asymmetric hydrogenation of functionalized double bonds, *Angew. Chem. Int. Ed.* 38 (1999) 3212–3215.
- [10] B.L. Feringa, R. Badorrey, D. Pena, S.R. Harutyunyan, A.J. Minnaard, Copper-catalyzed asymmetric conjugate addition of Grignard reagents to cyclic enones, *Proc. Natl. Acad. Sci. U. S. A.* 101 (2004) 5834–5838.
- [11] J. Deschamp, O. Riant, Efficient construction of polycyclic derivatives via a highly selective Cu-catalyzed domino reductive-aldo cyclization, *Org. Lett.* 11 (2009) 1217–1220.
- [12] R. Šebesta, F. Bilčík, P. Fodran, Enantioselective one-pot conjugate addition of Grignard reagents followed by a Mannich reaction, *Eur. J. Org. Chem.* (2010) 5666–5671.
- [13] Z. Galeštová, R. Šebesta, Diastereoselective Mannich reaction of chiral enolates formed by enantioselective conjugate addition of Grignard reagents, *Eur. J. Org. Chem.* (2011) 7092–7096.
- [14] F. Bilčík, M. Drusan, J. Marák, R. Šebesta, Enantioselective one-pot conjugate addition of Grignard reagents to cyclic enones followed by amidomethylation, *J. Org. Chem.* 77 (2012) 760–765.
- [15] J. Deschamp, T. Hermant, O. Riant, An easy route toward enantio-enriched polycyclic derivatives via an asymmetric domino conjugate reduction–aldo cyclization catalyzed by a chiral Cu(I) complex, *Tetrahedron* 68 (2012) 3457–3467.
- [16] J. Deschamp, O. Chuzel, J. Hannouche, O. Riant, Highly diastereo- and enantioselective copper-catalyzed domino reduction/aldo reaction of ketones with methyl acrylate, *Angew. Chem. Int. Ed.* 45 (2006) 1292–1297.
- [17] J. Ou, W.-T. Wong, P. Chiu, Reductive aldol cyclizations of unsaturated thioester derivatives of 1,3-cyclopentanedione catalyzed by chiral copper hydrides, *Tetrahedron* 68 (2012) 3450–3456.
- [18] D. Tomita, K. Yamatsugu, M. Kanai, M. Shibasaki, Enantioselective synthesis of SM-130686 based on the development of asymmetric Cu(I)F catalysis to access 2-oxindoles containing a tetrasubstituted carbon, *J. Am. Chem. Soc.* 131 (2009) 6946–6948.
- [19] F. Lopez, A.W. van Zijl, A.J. Minnaard, B.L. Feringa, Highly enantioselective Cu-catalysed allylic substitutions with Grignard reagents, *Chem. Commun.* (2006) 409–411.
- [20] S. Guduguntla, M. Fañanás-Mastral, B.L. Feringa, Synthesis of optically active β - or γ -Alkyl-substituted alcohols through copper-catalyzed asymmetric allylic alkylation with organolithium reagents, *J. Org. Chem.* 78 (2013) 8274–8280.
- [21] T. den Hartog, B. Maciá, A.J. Minnaard, B.L. Feringa, Copper-catalyzed asymmetric allylic alkylation of halocrotonates: efficient synthesis of versatile chiral multifunctional building blocks, *Adv. Synth. Catal.* 352 (2010) 999–1013.
- [22] M. Pérez, M. Fañanás-Mastral, P.H. Bos, A. Rudolph, S.R. Harutyunyan, B.L. Feringa, Catalytic asymmetric carbon–carbon bond formation via allylic alkylations with organolithium compounds, *Nat. Chem.* 3 (2011) 377–381.
- [23] T. Ireland, K. Tappe, G. Grossheimann, P. Knochel, Synthesis of a new class of chiral 1,5-diphosphanylferrocene ligands and their use in enantioselective hydrogenation, *Chem. Eur. J.* 8 (2002) 843–852.
- [24] N. Yoshikawa, L. Tan, J.C. McWilliams, D. Ramasamy, R. Sheppard, Catalytic enantioselective hydrogenation of N-alkoxy carbonyl hydrazones: a practical synthesis of chiral hydrazines, *Org. Lett.* 12 (2010) 276–279.
- [25] L.-B. Luo, D.-Y. Wang, X.-M. Zhou, Z. Zheng, X.-P. Hu, Asymmetric synthesis of 2-alkyl-3-phosphonopropanoic acid derivatives via Rh-catalyzed asymmetric hydrogenation, *Tetrahedron Asymmetry* 22 (2011) 2117–2123.
- [26] D. Scharschmidt, H. Lang, Selective syntheses of planar-chiral ferrocenes, *Organometallics* 32 (2013) 5668–5704.
- [27] L.F. Battelle, R. Bau, G.W. Gokel, R.T. Oyakawa, I.K. Ugi, Stereoselective synthesis. VIII. Absolute configuration of a 1,2-disubstituted ferrocene derivative with planar and central elements of chirality and the mechanism of the optically active α -ferrocenyl tertiary amines, *J. Am. Chem. Soc.* 95 (1973) 482–486.
- [28] I.R. Butler, W.R. Cullen, F.G. Herring, N.R. Jagannathan, α -N,N-Dimethylaminoethylferrocene. A nuclear magnetic resonance study relating to stereoselective metalation, *Can. J. Chem.* 64 (1986) 667–669.
- [29] R. Šebesta, A. Almásy, I. Čisárová, Š. Toma, New [5]ferrocenophane diphosphine ligands for Pd-catalyzed allylic substitution, *Tetrahedron Asymmetry* 17 (2006) 2531–2537.
- [30] A. Almásy, A. Škvorcová, B. Horváth, F. Bilčík, V. Bariak, E. Rakovský, R. Šebesta, Explanation of different regioselectivities in the ortho-lithiation of ferrocenyl(phenyl)methanamines, *Eur. J. Org. Chem.* (2013) 111–116.
- [31] O. Riant, G. Argouarch, D. Guillaneux, O. Samuel, H.B. Kagan, A straightforward asymmetric synthesis of enantiopure 1,2-disubstituted ferrocenes, *J. Org. Chem.* 63 (1998) 3511–3514.
- [32] M. Lotz, K. Polborn, P. Knochel, New ferrocenyl ligands with broad applications in asymmetric catalysis, *Angew. Chem. Int. Ed.* 41 (2002) 4708–4711.
- [33] K. Tappe, P. Knochel, New efficient synthesis of taniaphos ligands: application in ruthenium- and rhodium-catalyzed enantioselective hydrogenations, *Tetrahedron Asymmetry* 15 (2004) 91–102.
- [34] W. Chen, S.M. Roberts, J. Whittall, A. Steiner, An efficient and highly stereoselective synthesis of new P-chiral 1,5-diphosphanylferrocene ligands and

- their use in enantioselective hydrogenation, *Chem. Commun.* (2006) 2916–2918.
- [35] S.-i. Fukuzawa, M. Yamamoto, S. Kikuchi, Unexpected 1,5-dilithiation of chiral o-TMS blocked (Dimethylamino)phenylmethylferrocene: an alternative approach to chiral ferrocenyl 1,5-diphosphphanes, *J. Org. Chem.* 72 (2007) 1514–1517.
- [36] S.-i. Fukuzawa, M. Yamamoto, M. Hosaka, S. Kikuchi, Preparation of chiral homoannularly bridged N,P-ferrocenyl ligands by intramolecular coupling of 1,5-dilithioferrocenes and their application in asymmetric allylic substitution reactions, *Eur. J. Org. Chem.* (2007) 5540–5545.
- [37] X.-p. Hu, H.-l. Chen, X.-q. Hu, H.-c. Dai, C.-m. Bai, Z. Zheng, Novel Synthesis of Knochel'S Diphosphine Ligand and its Application in Pd-Catalyzed Asymmetric Allylic Alkylation, *J. Mol. Catal. (China)* 17 (2003) 279–281.
- [38] K. Yamamoto, J. Wakatsuki, R. Sugimoto, Modification of N,N-dimethyl-1-[(R)-1',2'-bis(diphenylphosphino)ferrocenyl]ethylamine (BPPFA) as a ligand for asymmetric hydrogenation of olefins catalyzed by a chiral rhodium(I) complex, *Bull. Chem. Soc. Jpn.* 53 (1980) 1132–1137.
- [39] A.L. Thompson, D.J. Watkin, CRYSTALS enhancements: absolute structure determination, *J. Appl. Cryst.* 44 (2011) 1017–1022.
- [40] H.D. Flack, M. Sadki, A.L. Thompson, D.J. Watkin, Practical applications of averages and differences of Friedel opposites, *Acta Cryst. Sec. A* 67 (2011) 21–34.
- [41] R.W.W. Hooft, L.H. Straver, A.L. Spek, Determination of absolute structure using Bayesian statistics on Bijvoet differences, *J. Appl. Cryst.* 41 (2008) 96–103.
- [42] F. Caprioli, M. Lutz, A. Meetsma, A.J. Minnaard, S.R. Harutyunyan, Structural characterisation of Cu complexes of chiral ferrocenyl diphosphine ligands, *Synlett* 24 (2013) 2419–2422.
- [43] J. Ou, W.-T. Wong, P. Chiu, Desymmetrizing reductive aldol cyclizations of enethioate derivatives of 1,3-diones catalyzed by a chiral copper hydride, *Org. Biomol. Chem.* 10 (2012) 5971–5978.
- [44] G.A. Jeffrey, An Introduction to Hydrogen Bonding, Oxford University Press USA, New York, 1997.
- [45] P. Van Der Sluis, A.L. Spek, BYPASS: an effective method for the refinement of crystal structures containing disordered solvent regions, *Acta Cryst. Sec. A* 46 (1990) 194–201.
- [46] S. Parsons, H.D. Flack, T. Wagner, Use of intensity quotients and differences in absolute structure refinement, *Acta Cryst. Sec. B* 69 (2013) 249–259.
- [47] CrysAlis Pro, 1.171.37.33, Agilent Technologies UK Ltd, 2014, Oxford, UK.
- [48] O.V. Dolomanov, L.J. Bourhis, R.J. Gildea, J.A.K. Howard, H. Puschmann, OLEX2: a complete structure solution, refinement and analysis program, *J. Appl. Cryst.* 42 (2009) 339–341.
- [49] P.W. Betteridge, J.R. Carruthers, R.I. Cooper, K. Prout, D.J. Watkin, CRYSTALS version 12: software for guided crystal structure analysis, *J. Appl. Cryst.* 36 (2003) 1487.
- [50] R.I. Cooper, A.L. Thompson, D.J. Watkin, CRYSTALS enhancements: dealing with hydrogen atoms in refinement, *J. Appl. Cryst.* 43 (2010) 1100–1107.
- [51] G.M. Sheldrick, A short history of SHELX, *Acta Cryst. A* 64 (2008) 112–122.